

Reply to “Interactive comment on “The vertical variability of ammonia in urban Beijing, China” by Yangyang Zhang et al.” (Referee #2 in RC1)

General Comments

5 This manuscript describes one year’s worth of weekly integrated ammonia concentrations at 16 levels between 2m and 320m above ground on a tower in metropolitan Beijing. Concentrations were comparatively high throughout the year, highest in summer and, on average, a bit less than half the summer values in winter. A source allocation exercise indicated both local (urban) and regional (agricultural) influences. The profiles showed relatively little variation in the vertical, suggesting
10 a well-mixed boundary layer much of the time, or smearing of more detailed features due to integrating over a week with passive samplers, or most likely a combination of both.

The paper is well written, concise, and addresses a topic of increasing interest to the community, namely ammonia in the atmosphere. Sufficient material is presented to substantiate the conclusions, and proper credit is given to previously
15 published work. The authors are aware of the limitations of weekly integrated passive samples, but nevertheless provided a useful data set that deserves to be published. The reported ammonia concentrations certainly have the potential to play a significant role in the atmospheric chemistry over Beijing, and the added
20 details of the vertical distribution in the boundary layer and potential source regions is useful information.

Re: Thank you for your valuable comments and appreciation of our study. We have made the suggested changes and corrections in the revision. We respond in detail to the questions and comments below (in blue).

Specific comments

25 Line 20: a bit convoluted. Rephrase to “the highest seasonal NH₃ concentrations across the profile were observed in summer (), followed by spring () ...”

Re: We have rephrased the sentence as suggested.

L35: "In China, annual ...".

30 Re: We have made this change.

L35: European plus US?

Re: During 1990-2005, annual NH₃ emissions in China were 2 and 3 times higher than Europe and the US, respectively. The expression was corrected in the revised manuscript.

35 L89: how are the 10 million defined? The number of distinct vehicles multiplied by the number of trips for each per day, integrated around the whole ring road?

Re: Daily traffic volumes of 10 million for both ring roads around the sampling site (IAP tower) are cited from Pan et al. (2016), reasonably representing the number of passengers. The number was updated in the revised manuscript by using an official data of traffic volumes for Beijing ring roads in 2016 (Beijing Transport Institute, 2017). The sentence was thus revised as "The site is approximately 0.8 km north of the third Ring Road, 1.3 km south of the fourth Ring Road and 0.2 km west of the Beijing-Tibet expressway, major transport arteries encircling Beijing, each with average traffic volumes of over 200,000 vehicles day⁻¹ in 2016 (Beijing Transport Institute, 2017), representing a typical urban site surrounded mainly by residential areas."

45 References:

1. Pan, Y., Tian, S., Liu, D., Fang, Y., Zhu, X., Zhang, Q., Zheng, B., Michalski, G., and Wang, Y.: Fossil fuel combustion-related emissions dominate atmospheric ammonia sources during severe haze episodes: Evidence from ¹⁵N-stable isotope in size-resolved aerosol ammonium, *Environmental Science & Technology*, 50, 8049, 2016.

2. Beijing Transport Institute: Annual report of Beijing traffic development in 2017, <http://www.bjtrc.org.cn/JGJS.aspx?id=5.2&Menu=GZCG>, 2017.

55 L99: add a sentence to explain how the MDL is defined mathematically.

Re: MDL was calculated using the following equation: $MDL \geq t \times S_b \times \sqrt{\frac{N_1 + N_2}{N_1 \times N_2}}$, t value given at the 95% confidence level for the appropriate of degrees of freedom, S_b is the blank standard deviation, N_1 and N_2 is the number of sample measurements (single measurement, $N_1=1$), the number of analyzed blanks.
60 Updated in the revised manuscript.

L102: add a sentence to this paragraph that explains how particle NH_4^+ is kept from the ALPHA sampling medium.

Re: We have added: "The samplers operate on the principle of diffusion using an acid-coated filter to capture the ammonia. A PTFE (Teflon) membrane is placed
65 directly at the mouth of the sampler, forming a quiescent boundary layer in front of the sample membrane. A stable, turbulent-free diffusion path length is achieved behind the membrane, whilst allowing gaseous ammonia to diffuse through for capture and minimizing the sampling of NH_4^+ aerosol (Tang et al., 2014)."

Reference:

70 1. Tang, Y. S., Cape, J. N., and Sutton, M. A.: Development and types of passive samplers for monitoring atmospheric NO_2 and NH_3 concentrations, Scientific World Journal, 1, 513-529, <https://doi.org/10.1100/tsw.2001.82>, 2014.

L143: check your numbers; from Fig. S3, the winter percentage looks more like 23%.

75 Re: Thank you. We have check to make sure the numbers are consistent between Figure S3 and the numbers in the text.

L159: remove "higher"

Re: Done.

L167: a convoluted sentence. Please rephrase.

80 Re: The sentence was revised as: "Some seasonal variations were observed, i.e.

the frequency of high NH₃ concentration was greater with southerly winds than northwesterly winds in the spring, increased frequency of high NH₃ concentrations were associated with southerly and easterly winds in the summer and autumn, and NH₃ concentrations still exceeded 5 µg m⁻³ during winter with relatively frequent winds from the northwest."

85

L177: their instead of there?

Re: Corrected.

L205: an additional factor for the straighter profile near the ground is the larger surface roughness in an urban area, vs. the fields around the BAO tower, causing stronger mixing.

90

Re: Thank you for your comment. The related expression was added in the revised manuscript - "In contrast to the "rural" boundary layer above the fields surrounding the BAO tower, the mixing in the Beijing urban area could be greatly enhanced by larger surface roughness and surface heating (Baklanov and Kuchin, 2004)."

95

Reference:

1. Baklanov, A. and Kuchin, A.: The mixing height in urban areas: comparative study for Copenhagen, Atmos. Chem. Phys. Discuss., 4, 2839-2866, <https://doi.org/10.5194/acpd-4-2839-2004>, 2004.

Table 1: is it possible / would it make sense to add the Zhou et al. (2017) results to this table, since they are from the same tower?

100

Re: We agree and have added the data from Zhou et al (2017).

Fig. 1: I would change the scale to kg/km²/yr for increased portability

Re: We have made this change in the revised manuscript.

Fig. 3: add a big "Beijing" label near the top row and "BAO" near the bottom row for easier identification

105

Re: Done in the revised manuscript.

Fig. S4: state the units of the slopes

Re: We have added the units of the slope to the x axis label.

110 Fig. S6: from years of experience seeing people averaging wind directions
incorrectly, windroses that look like this always immediately cause me concern!
There seem to be almost no winds from the north. Sometimes, this is an artifact of
simply arithmetically averaging wind directions, which results in many northerly
winds showing up as southerly instead (since the average of 355 and 5 is 180, for
example). The proper way to do this of course is a vector decomposition into
115 easterly and northerly wind components before averaging these and then
calculating the average wind direction. Please confirm that wind directions have
been averaged properly here.

120 Re: Thank you for your suggestion. We fully agreed with you. Wind direction was
collected hours from the sensor. An internal program in the met station correctly
averages the wind direction to hourly values. Actually, hourly wind directions were
used in Fig. S6 (windroses), which was not supposed to cause any incorrect wind
direction frequency during the calculation.

The vertical variability of ammonia in urban Beijing, China

Yangyang Zhang¹, Aohan Tang^{1,*}, Dandan Wang¹, Qingqing Wang², Katie Benedict³, Lin Zhang⁴,
Duanyang Liu⁵, Yi Li⁶, Jeffrey L. Collett Jr.³, Yele Sun^{2,Z*}, Xuejun Liu^{1,*}

¹Beijing Key Laboratory of Farmland Soil Pollution Prevention and Remediation, College of Resources and Environmental Sciences, China Agricultural University, Beijing 100193, China

²State Key Laboratory of Atmospheric Boundary Layer Physics and Atmospheric Chemistry, Institute of Atmospheric Physics, Chinese Academy of Sciences, Beijing 100029, China

³Department of Atmospheric Science, Colorado State University, Fort Collins, CO80523, USA

⁴Laboratory for Climate and Ocean-Atmosphere Studies, Department of Atmospheric and Oceanic Sciences, School of Physics, Peking University, Beijing 100871, China

⁵Jiangsu Meteorological Observatory, Nanjing 210008, China

⁶Sunset CES Inc., Beaverton, OR97008, USA

⁷[Collaborative Innovation Center on Forecast and Evaluation of Meteorological Disasters, Nanjing University of Information Science & Technology, Nanjing 210044, China](#)

*Corresponding authors (aohantang@cau.edu.cn, sunyele@mail.iap.ac.cn, liu310@cau.edu.cn)

Abstract. Weekly vertical profiles of ammonia (NH₃) were measured at 16 heights on the Beijing 325 m meteorological tower for one year from March 2016 to March 2017. ~~Measured The~~ average NH₃ concentrations ~~at all heights~~ exceeded ~~5-4~~ $\mu\text{g m}^{-3}$ ~~at all heights~~ with an overall average ($\pm 1\sigma$) ~~tower concentration value~~ of $13.3 (\pm 4.8) \mu\text{g m}^{-3}$. The highest NH₃ concentrations along the vertical profiles mostly occurred at 32-63 m, decreasing both towards the surface and at higher altitudes. Significant decreases in NH₃ concentrations were only found at the top two heights (280 and 320 m). These results suggest an ~~NH₃ ammonia~~ rich atmosphere during all seasons in urban Beijing, from the ground to at least 320 m. ~~Highest concentrations were observed in summer, associated with high temperature.~~ The ~~highest average seasonal~~ NH₃ concentrations ~~across the profile~~ ~~were from high to low~~ was observed in summer ($18.2 \mu\text{g m}^{-3}$) ~~with high temperature~~, followed by spring ($13.4 \mu\text{g m}^{-3}$), autumn ($12.1 \mu\text{g m}^{-3}$), and winter ($8.3 \mu\text{g m}^{-3}$). ~~Significant vertical variation of NH₃~~

带格式的: 到齐到网格

带格式的: 英语(英国)

带格式的: 突出显示

concentration was only found in summer. Source region Transport analyses suggest that air masses arriving from intensive agricultural regions to the south contribute most to the high NH₃ concentrations in Beijing. Local sources such as traffic emissions also appear to be important contributors to atmospheric NH₃ in this urban environment.

1. Introduction

Ammonia (NH₃) has long been recognized as an important form of reactive nitrogen (Nr) in atmospheric environment, playing a key role in biogeochemical cycles from atmospheric chemical processes to deposition and subsequent environmental impacts (e.g. air pollution, reduced biodiversity, acidification, and eutrophication) (Fowler et al., 2009; Sutton et al., 2008). NH₃ reacts with nitric and sulfuric acids in air, forming secondary inorganic aerosols (e.g., NH₄NO₃, (NH₄)₂SO₄) with long atmospheric lifetimes that can transport these species far from sources and contribute 40-57% of fine particle matter in megacities (Fowler et al., 2009; Huang et al., 2014; Yang et al., 2011). Therefore, NH₃ has received increasing attention in air pollution research (Wang et al., 2015). In addition to agriculture, which is considered the largest NH₃ source globally, emissions from biomass burning, industries, vehicles, and other sources (Galloway et al., 2003; Sutton et al., 2008; Erisman et al., 2008; Sun et al., 2016; Sun et al., 2017) can also be significant.

In China, annual NH₃ emissions were approximately 2- and 3 times higher than European and US emissions, respectively, over the period 1990 to 2005 (Reis et al., 2009; Kang et al., 2016; Zhao and Wang, 1994; Klimont, 2001; EMEP; USEPA, 2009), and estimated at 14.6 Tg N yr⁻¹ in 2010 (Liu et al., 2013) and 15.6 Tg N yr⁻¹ in 2015 (Zhang et al., 2017) (Reis et al., 2009; Kang et al., 2016; Zhao and Wang, 1994; Klimont, 2001; EMEP; USEPA, 2009; Zhang et al., 2017). Such high emissions, together with the important role NH₃ plays in degrading air quality, makes NH₃ a key target to curb serious air pollution in Chinese urban areas (Fu et al., 2017; Chang et al., 2016; Ye et al., 2011; Wang et al., 2011). Some studies have indicated that reducing NH₃ concentrations could be an effective method for alleviating secondary inorganic PM_{2.5} pollution in China (Gu et al., 2014; Wang et al., 2015; Wu et al., 2016; Xu et al., 2017). However, NH₃ has been received less attention from the government, however, than SO₂ and NO_x, which have been controlled since 2005 and been effectively reduced during the 12th Five-Year Plan period (2011-2015) (Fu et al., 2017).

带格式的: 突出显示

带格式的: 突出显示

带格式的: 突出显示

175 Currently there are strong arguments about the role of regional transport in contributing to haze pollution in China (Guo et al., 2014; Li et al., 2015), especially for severe haze episodes occurring during stagnant meteorological conditions with a shallow boundary layer (Sun et al., 2014; Zheng et al., 2015; Quan et al., 2013). Vertical characterization of air pollutant concentration profiles may be helpful for elucidating factors contributing to the formation and transport of regional haze events (Quan et al., 2013; Tang et al., 2015; Wiegner et al., 2006). Many studies have been conducted to improve our understanding of temporal and spatial concentration dynamics of atmospheric NH₃ and how they relate to underlying factors (e.g. emission intensity, meteorological conditions, etc.) and air quality (Yamamoto et al., 1988; Yamamoto et al., 1995; Bari et al., 2003; Vogt et al., 2005; Lee et al., 1999). However, such studies in China have generally focused on the spatial distribution of NH₃ near the ground (Ianniello et al., 2010; Wu et al., 2009; Meng et al., 2011; Xu et al., 2015) and
180 the vertical characterization of NH₃ concentrations is very limited.

As a trace gas with both point and non-point sources, as well as a tendency to deposit rapidly to surfaces, NH₃ mixing ratios may vary significantly as a function of height. In urban locations, like Beijing, where NH₃ is a key contributor to fine particle formation, local (~~e.g., traffic~~) sources (e.g., traffic) emit at the surface and are then mixed through the boundary layer, while NH₃ transported from agricultural sources outside the city ~~are is~~ presumably already mixed through
185 the boundary layer. The influence of these behaviors may be reflected in vertical NH₃ concentration gradients measured within the city. For example, dominant local surface traffic emissions might give rise to a profile that peaks near the surface, while ~~NH₃ ammonia~~ transported into the urban area may be uniformly mixed in the vertical or even decline near the surface due to loss by dry deposition. Of course these patterns are expected to be further affected by sinks, including surface deposition as well as fine particle formation of ammonium salts. NH₃ vertical distribution measurements are also
190 useful for advancing satellite retrievals, which offer a great potential for understanding the global distribution of gaseous NH₃ (Shephard and Cady-Pereira, 2015; Sun et al., 2015; Van Damme et al., 2015).

To our knowledge there are few studies reporting long-term observations of vertical distributions of NH₃ in the lowest few hundred meters of the atmosphere, including measurements at the BAO tower in the USA (Li et al., 2017; Tevlin et al., 2017) and CESAR in The Netherlands (Dammers et al., 2017). Li et al. (2017) analyzed vertical NH₃ concentration
195 profiles at the BAO tower in Colorado, USA, reporting the minimum concentration at the top of the tower, slowly

increasing towards a peak concentration at ~10 m before a large reduction in concentration at 1 m. The site was influenced by transport of high ammonia-NH₃ concentrations from large animal feeding operations to the northeast. Through higher time resolution measurements at the BAO tower, Tevlin et al. (2017) pointed out that the surface can act as an occasional NH₃ sink as well as a source. The CESAR study in the Netherlands showed that vertical profile differences were mainly due to local and regional transport influences (Dammers et al., 2017)(Li et al., 2017). Because the BAO and CESAR tower sites are both located in a-suburban areas with low aerosol mass loadings, observed vertical profiles of aerosol and gas species (Öztürk et al., 2013; VandenBoer et al., 2013; Riedel et al., 2013) could be substantially different from those in megacities in China. Zhou et al. (2017) measured vertical concentration profiles of NH₃ and seven other air pollutants at ten heights (8, 15, 47, 80, 120, 160, 200, 240, 280 and 320 m) in urban Beijing, finding NH₃ concentrations peaked at 160 m. However, ~~only one vertical profile was measured the observation period was too short (two weeks) to investigate seasonal variations~~ and may not adequately represent typical conditions. Until now, long-term monitoring of vertical NH₃ concentration profiles has not been carried out in China.

Here, we report a one-year field campaign on the Beijing 325 m meteorological tower to investigate vertical NH₃ concentration profiles and consider how temporal variations may relate to urban emission sources, meteorological factors and air transport from more distant sources. Study findings are relevant for our understanding of precursor NH₃ammonia distributions and the role of NH₃ammonia in the formation of severe aerosol pollution in China, and further provide benchmarks to assist in meeting air quality goals and policy needs in future.

2. Materials and methods

2.1 Site Description

The sampling site is located at the State Key Laboratory of Atmospheric Boundary Layer Physics and Atmospheric Chemistry (LAPC), Institute of Atmospheric Physics (IAP), Chinese Academy of Sciences (CAS) in urban Beijing (39°58' N, 116°22'E) (Fig. 1). The site is approximately 0.8 km north of the third Ring Road ~~and~~, 1.3 km south of the fourth Ring Road ~~and 0.2 km west of the Beijing-Tibet expressway, which are three major~~ transport arteries encircling Beijing, each

带格式的: 下标

with average traffic volumes of approximately over 200,000+ million vehicles day⁻¹ in 2016 (Beijing Transport Institute, 2017), representing a typical urban site surrounded mainly by residential areas.

2.2 NH₃ measurement

From March 16, 2016 to March 16, 2017, weekly atmospheric NH₃ samples were collected at 16 heights on the 325 m meteorological tower using ALPHA passive samplers (adapted low-cost high absorption, Centre for Ecology and Hydrology, Edinburgh, UK) except for a few samples with slightly different duration due to tower the maintenance -of the towerschedules. The samplers operate on the principle of diffusion using an acid-coated filter to capture the NH₃ammonia. A PTFE (Teflon) membrane is placed directly at the mouth of the sampler, formatting a quiescent minimized-boundary layer in front of the sample membrane. Hence, a stable, turbulent-free diffusion path length is achieved behind the membrane, whilst allowing gaseous NH₃ammonia to diffuse through for capture and minimizing the sampling of NH₄⁺aerosol (Tang et al., 2014). NH₃ was sampled at 2, 8, 15, 32, 47, 63, 80, 102, 120, 140, 160, 180, 200, 240, 280, and 320 m above ground level. At each height, three ALPHA samplers were deployed under a PVC shelter to protect the samplers from rain and direct sunlight (shown in Fig. 1). Collected NH₃ samplers were extracted with 10 mL high-purity water (18.2 MΩ-cm) and analyzed using a continuous-flow analyzer (Seal AA3, Germany). Three field (travel) blanks were prepared for each batch of samples, analyzed together with those samples, and used to blank correct sample results and determine the minimum-method detection limits (MDL). MDL was calculated using the following equation: $MDL \geq t \times S_b \times \sqrt{\frac{N_1 + N_2}{N_1 \times N_2}}$. t value given at the 95% confidence level for the appropriate of degrees of freedom, S_b is the blank standard deviation, N_1 and N_2 is the number of sample measurements (single measurement, $N_1=1$), the number of analyzed blanks using standard deviation of NH₃ concentrations for blank samples multiplied versus the determined one-sided t-distribution for a 95% confidence level. From the field blanks, the MDL was calculated to be 0.31 μg m⁻³ for a one-week ALPHA passive NH₃ sample. All lab measurements were conducted in the Key Laboratory of Plant-Soil Interactions, Chinese Ministry of Education, China Agricultural University. More details of the passive samplers and related laboratory preparation and analysis can be found in Xu et al. (2015).

带格式的：下标

带格式的：上标

带格式的：下标

带格式的：下标

带格式的：下标

带格式的：下标

带格式的：下标

带格式的：下标

2.3 Meteorological data

Meteorological parameters, including wind speed (WS), wind direction (WD), relative humidity (RH), and temperature (T), were obtained at all sampling heights except 2 m, and the temperature was not available at 8 m. WS and WD were measured using four-cup anemometers (model O10C, Met One Instruments), and RH and T were measured using a T /RH sensor (model HC2-S3, ROTRONIC).

2.4 Data analysis

Repeated-measures analysis of variance (ANOVA) was used to test changes in NH_3 concentration along vertical profiles. When the ANOVA results were significant, the Tukey's Honest Significant Difference (HSD) test was used to determine the significance of the difference between means with a significance level of $P < 0.05$. The coefficient of determination was used to test the linear correlations with a significance level of $P < 0.05$. All the statistical analyses were conducted using SPSS Version 23.0 (IBM Corp., Armonk, NY, USA).

Potential source contribution function analysis (PSCF) (Ashbaugh et al., 1985) of atmospheric NH_3 was performed using Meteoinfo (TrajStat package) (Wang, 2014), where 72 h back trajectories arriving at the monitoring site (IAP tower) at each height were calculated every 3 h for the entire study period. The average NH_3 concentration for each cluster was computed using the cluster statistics function. NH_3 pathways could then be associated with the high concentration clusters. The number of trajectory segment endpoints falling in a grid cell (i, j) is n_{ij} . The number of trajectory endpoints associated with the data with the concentration of NH_3 concentrations higher than an arbitrarily set criterion for each height during the four seasons (75th percentile for NH_3 was set here) is m_{ij} (Table S1). The PSCF value for the ij^{th} cell is then calculated as m_{ij}/n_{ij} . A weighting function W_{ij} was applied to reduce the uncertainties of small values of n_{ij} (Polissar et al., 1999). Weighted PSCF values (WPSCF) were calculated by multiplying a particular W_{ij} (≤ 1.00) if the total number of the endpoints for one grid cell was lower than three times the average of the endpoints per each cell. Higher WPSCF values indicate higher potential contributions of NH_3 to the receptor site (IAP tower).

带格式的: 字体: 倾斜

带格式的: 字体: 倾斜

带格式的: 字体: 倾斜

带格式的: 字体: 倾斜

带格式的: 字体: 倾斜

带格式的: 突出显示

$$w_{ij} = \begin{cases} 1.00 & 80 < n_{ij} \\ 0.70 & 20 < n_{ij} \leq 80 \\ 0.42 & 10 < n_{ij} \leq 20 \\ 0.05 & n_{ij} \leq 10 \end{cases}$$

265 3. Results

3.1 Vertical profiles of NH₃ concentrations

The time series of weekly averages of NH₃ concentrations during March 16, 2016 - March 16, 2017 are shown in Fig. 2.

The weekly NH₃ concentration across all heights averaged 13.3±4.8 μg m⁻³ during the year-long study period. Individual weekly concentrations ranged from 4.4 μg m⁻³ at 2 m to 25.3 μg m⁻³ at 32 m. **Nearly all (99.6%)** of the weekly NH₃

270 concentrations along the profile exceeded 5 μg m⁻³. Summer concentrations were generally the highest. Maximum NH₃ concentrations mostly occurred between 32 m and 63 m, decreasing both towards the surface and the top of the tower. Minimum concentrations mostly occurred at 2 m and 320 m (Fig. S1). Significant differences of annual average NH₃ concentrations across the vertical profile were only found between the “maximum concentration” height and the top two heights, i.e. 280 m and 320 m (Fig. 3i). Even at 320 m, the annual average NH₃ concentration was still relatively high at 11.3 μg m⁻³ (Fig. 3i). During the whole **Beijing**-observation period, the daily average boundary layer height was generally above 320 m, indicating a good portion of the sampling occurred within a well-mixed boundary layer (Fig. S2).

280 Seasonal vertical concentration profiles exhibited fairly similar shapes ~~that were fairly similar to that of~~ the annual average profile, ~~but yet~~ with some important differences in absolute concentration values and the magnitude of vertical gradients within the profiles (Fig. 3). The average NH₃ concentration across the profile from high to low was observed in summer (18.2 μg m⁻³), spring (13.4 μg m⁻³), autumn (12.1 μg m⁻³), and winter (8.3 μg m⁻³). Proportional declines of NH₃ concentration from the peak to higher and lower elevations differed between seasons, being the greatest in autumn (28.31% decrease from 63 m to 320 m), and winter (27.23.8%) followed by **summer** (19.720.5%) and spring (15.48%) (Fig. S3).

带格式的: 突出显示

带格式的: 字体颜色: 自动设置

带格式的: 突出显示

3.2 Meteorological variability

285 Vertical NH₃ concentration profiles varied substantially during the sampling period, along with vertical changes in meteorological parameters. Bivariate polar plots (Fig. 4) show that high NH₃ concentrations below 47 m were mostly observed during periods with low wind speeds (< 4 m s⁻¹). As heights and associated wind speeds increased, the relationship between NH₃ concentrations and wind speed weakened. For example, at 280 m, the highest concentration was observed when the wind speed was also high (up to an average of ~15 m s⁻¹).

290 Wind directions play an important role in air pollution transport. Transport from the northwest was typically associated with low NH₃ concentrations at all heights, consistent with the absence of large emissions sources in the mountains NW of Beijing. It is noteworthy that high NH₃ concentrations at near-surface heights (8 m and 15 m) always coincide with winds from the south, including southeast and southwest directions. High NH₃ concentrations appear to be associated with winds from the northeast from 32 m until 80 m. Above 80 m, winds from the south contribute more
295 to high NH₃ concentrations. Major regions of agricultural NH₃ emissions are located south and east of Beijing.

To further investigate observed variability, we show the probability density function of NH₃ concentrations in relation to the relative humidity (RH) and temperature (T) (Fig. 5). Clear positive relationships between T and NH₃ concentrations were found at all heights from low RH to high RH. When T was low ($T < 12^\circ\text{C}$), the NH₃ concentration fell mostly below 10 $\mu\text{g m}^{-3}$ under any RH condition. The occurrence of high NH₃ concentrations increased with higher $T > 12^\circ\text{C}$, which is not
300 surprising, given that agricultural NH₃ emissions increase with T while higher T and lower RH also shift the equilibrium of the $\text{NH}_3(\text{g}) + \text{HNO}_3(\text{g}) \leftrightarrow \text{NH}_4\text{NO}_3(\text{p})$ system toward the gas phase. Statistically, a strong positive relationship was found between NH₃ and T at all heights from the surface to the top of the tower ($R^2 \sim 0.6$) (Fig. S4); both slope and correlation coefficients were similar across all heights. Although, a positive correlation between NH₃ and RH and a negative correlation between NH₃ and wind speed (WS) were found, the correlation coefficients were quite low.

305 3.3 Potential source analysis

Analysis of the relationship between local wind direction and NH₃ concentrations does not fully clarify the potential source regions contributing to observed NH₃ ammonia at the sampling site (Fig. S6). Some seasonal variations were observed

带格式的: 字体: 倾斜

带格式的: 字体: 倾斜

带格式的: 字体: 倾斜

带格式的: 字体: 倾斜

带格式的: 字体: 倾斜

带格式的: 字体: 倾斜

带格式的: 突出显示

带格式的: 突出显示

带格式的: 突出显示

带格式的: 字体: 倾斜

related to season, such as i.e. the frequency of high NH_3 concentration was higher greater with southerly winds than northwesterly winds increased as wind sectors changed from northwest to south in the spring, higher increased frequency of high NH_3 concentrations were associated with southerly and easterly winds in the summer and autumn, and NH_3 concentrations still exceeded $5 \mu\text{g m}^{-3}$ during winter with relatively frequent winds from north and the northwest.

To examine the relationship between air transport and NH_3 ammonia concentrations more rigorously, weighted PSCF (WPSCF) during the four seasons were calculated for several measurement heights (2, 63, 180, 320 m) (Fig. 6). In summer, from the surface to the tower top, a strong influence is seen from source areas to the south of Beijing, coinciding with regions (e.g. Tianjin, Henan, Hebei and Shandong provinces) characterized by elevated anthropogenic emissions of NH_3 (Fig. 1), largely from agricultural activities (Zhang et al., 2009; Gu et al., 2012). During summer, regions to the north and west of the monitoring site had low WPSCF values. High WPSCF values to the south and southeast were common during spring. High WPSCF values were mainly located northwest and southeast of Beijing in autumn, while there their WPSCF values were typically lower in winter than during other seasons.

It is important to remember that aerosol-gas partitioning can also strongly influence measured NH_3 concentrations. To investigate seasonal phase changes between NH_3 and NH_4^+ , we define the NH_3 ammonia gas fraction (F_{NH_3} = the gaseous NH_3 concentration divided by the sum of the gaseous NH_3 and fine particulate NH_4^+ concentrations), where the concentrations are expressed in molar units. Monthly average partitioning for these reduced inorganic nitrogen forms from a nearby urban monitoring site, 10 km away from the IAP tower, is plotted in Fig. S8. The NH_3 gas fraction (F_{NH_3}) was found to be the highest in summer (0.83 in August) and the lowest in winter (0.36 in February). As expected, gas phase NH_3 is favored in the warmer months, while particle phase NH_4^+ is favored for the cooler months, with a gradual transition. Weekly NH_4^+ concentrations at the tower were estimated using weekly NH_3 concentrations divided by monthly F_{NH_3} , then, WPSCF analysis of the sum of $\text{NH}_3 + \text{NH}_4^+$ was performed (see results in Fig. S9). Results of this total WPSCF ($\text{NH}_3 + \text{NH}_4^+$) analysis yielded similar patterns to the NH_3 WPSCF analysis for all heights and seasons, indicating the importance of the identified source regions for both the gaseous and particulate atmospheric forms of emitted NH_3 .

带格式的: 下标

4. Discussion

4.1 Vertical NH₃ concentration profiles

The North China Plain is a well-known “hotspot” for NH₃ emissions due to the rapid development of industrialization, urbanization and intensive agriculture (Kang et al., 2016; Zhang et al., 2010). In our study, high atmospheric NH₃ concentrations (13.3±4.8 µg m⁻³) were found up to 320 m above ground level in urban Beijing (March 16th, 2016 - March 16th, 2017), much higher than the average annual NH₃ concentration (3.3±1.4 µg m⁻³) observed across a vertical profile at the 300 m USA rural BAO tower (Li et al., 2017). Some studies of NH₃ vertical distribution found that the NH₃ concentration significantly decreased with height. For example, Tevlin et al. (2017) reported an overall increase in summertime NH₃ mixing ratios toward the surface of 6.7 ppb or 5.1 µg m⁻³ (89%) during the day and 3.9 ppb or 3.0 µg m⁻³ (141%) at night. In the BAO tower study (Li et al., 2017), which also measured concentrations using passive (Radiello) samplers deployed for one to two week sample periods, the concentration profiles showed a similar overall vertical distribution. The minimum NH₃ concentration was at the top, slowly increasing towards a peak concentration at ~10 m before a sharp reduction near the surface. By contrast, our results showed much smaller decreases in NH₃ concentrations in upper air in urban Beijing (Table 1), with only a 1.18 µg m⁻³ (9.5%) average decrease from the surface to the top (Fig. 3i). The flatter shape of the Beijing vertical profile may reflect a combination of strong local (e.g. vehicle) and regional (e.g. industrial and agricultural emissions) sources (Fig. 2 and Fig.6) in our study, the fact that deep mixing layers regularly enveloped the full height of the tower within the surface boundary layer so that all sources influencing the tower measurements were vertically well mixed (Fig. S2), and/or the averaging of more distinct profiles over the week-long sample periods. In contrast to the “rural” boundary layer above the fields surrounding the BAO tower, the mixing in the Beijing urban area could be greatly enhanced by larger surface roughness (e.g. average urban building height being ~50 m) and surface heating (Baklanov and Kuchin, 2004). Higher time resolution vertical profile measurements are needed in the future to untangle the influence of these potential factors.

Distinct seasonal variations in NH₃ concentrations were found (Fig. 2), statistically most strongly associated with temperature rather than relative humidity or wind speed (Fig. S4). High temperatures enhance NH₃ emissions from soil,

带格式的: 突出显示

带格式的: 突出显示

带格式的: 突出显示

355 applied fertilizers, ~~and~~ animal waste, ~~can enhance~~ vertical mixing, and increase volatilization of NH₃ from NH₄NO₃ particulate matter (Bari et al., 2003; Ianniello et al., 2010; Li et al., 2014; Lin et al., 2006; Meng et al., 2011; Plessow et al., 2005; Walker et al., 2004; Zbieranowski and Aherne, 2012). While high (low) mixed-layer heights in spring and summer (autumn and winter) could dilute (concentrate) NH₃ in the surface boundary layer (Fig. S3), average NH₃ concentrations across the profile were actually high in summer/spring and low in winter/autumn, consistent with the strong temperature-driven seasonal variation of NH₃ concentration and the greater NH₄NO₃ particle formation during cold periods in autumn and winter. ~~Conducting~~~~Having~~ simultaneous measurements of fine particle composition, ~~with at different heights~~, in future studies would be valuable for more closely evaluating the influence of changes in phase-partitioning.

360 Li et al. (2017) found (~~Fig. 3j~~) a vertical difference of approximately 75% from the concentration peak near the surface to the top of the BAO tower in winter (Fig. 3j), and attributed this strong vertical gradient to the occurrence of low level temperature inversions which trapped emissions closer to the surface in winter. During our study in Beijing, the vertical gradient was only 28% in winter (maximum concentration found at 32 m), consistent with a deeper average boundary layer. Inversions, however, did limit vertical mixing of NH₃ during some periods in Beijing. Examination of thermal inversion layer probability at 6 a.m. and 3 p.m. (Fig. S7b and 7c) revealed that T inversions (0.22±0.26 °C) frequently occurred between 102 m and 160 m. Consequently, persistent higher NH₃ concentrations begin at a lower altitude (Fig. S7a) as also observed by Tevlin et al. (2017). Because the time resolution of our Beijing study was one sample per week, we could not catch the changes between the daytime and nighttime NH₃ vertical mixing. Compared to NH₃ monitoring in real time (Tevlin et al., 2017), weekly sampling smooths diurnal vertical distributions and makes it harder to identify the influence of local, surface sources or sinks.

375 Surfaces can act either as sources or sinks of NH₃, depending on surface NH₃ content, ambient NH₃ concentrations, ~~and~~ local meteorology and surface type (Tevlin et al., 2017; Zhang et al., 2010). The maximum NH₃ concentration occurrence at 2 m in Beijing and the concentration decrease with increased height may reflect an important surface source of NH₃, although our limited time resolution makes such conclusions tentative. The influence of evaporation of dew/precipitation may also be important. Some studies found that dew is both a significant night-time reservoir/sink and strong morning source of NH₃ (Wentworth et al., 2016; Teng et al., 2017).

带格式的: 字体: 倾斜

带格式的: 突出显示

带格式的: 突出显示

380 4.2. Potential source analysis

Areas south of Beijing with high WPSCF values appear to be important NH₃ source regions (Fig. 6), suggesting regional transport from high agricultural NH₃ emission areas (e.g. Hebei, Henan, Shandong provinces etc.) contributed significantly to atmospheric NH₃ in the Beijing urban region. Consistently higher NH₃ concentrations were observed during periods with winds from the SE, S and SW at all heights, especially in summer (Fig. S6). Although NH₃ has a limited atmospheric
385 lifetime with respect to dry deposition, concentrations in these agricultural NH₃ source regions can be extremely high (Shen et al., 2011) while significant ~~NH₃ ammonia~~ can be tied up in longer-lived ammonium nitrate particles that partially dissociate to release NH₃ back to the gas phase in response to NH₃ loss by dry deposition (Ianniello et al., 2011; Kang et al., 2016; Xu et al., 2017). The WPSCF (Fig. 6) and NH₃ emissions distribution (Fig. 1 left) both suggest the importance not only of regional transport from nearby areas, but also the potential for local emissions to play an important role in
390 sustaining the high NH₃ level in Beijing, e.g. vehicular traffic (Chang et al., 2018; Pan et al., 2018a). As discussed above, stagnant meteorological conditions with low WS and ~~T inversions allow local emissions, such as those from urban traffic,~~ to accumulate. Additionally, the topography of the mountains to the west and north of Beijing effectively traps polluted air over Beijing during southerly airflow, an effect reported in many Beijing particulate matter studies (Xia et al., 2016; Wu et al., 2009; Zhao et al., 2009).

395 Generally, NH₃ source regions identified in WPSCF analysis (Fig. 6) suggested that regional transport from the south exerts an important influence on Beijing NH₃ concentrations throughout the year. The area south of Beijing (e.g. Hebei, Henan and Shandong provinces) is a hotspot of NH₃ emission (Zhang et al., 2018) and half of NH₃ emissions have been estimated to deposit as NH₃ at urban sites in North China Plain (Pan et al., 2018b). In addition, seasonal patterns of NH₃ potential sources (Fig. 6) matched well with the seasonal surface NH₃ concentrations in China (Zhang et al., 2018). In
400 detail, NH₃ concentrations were typically highest in summer and south winds produced higher NH₃ concentrations than other ~~summer~~-wind directions (Fig. S6). Spring and summer had a similar wind direction distribution (Fig. S6) and wind speeds (Fig. S5), but corresponding NH₃ concentrations were lower in spring. This may reflect decreased emissions in regions to the south during cooler spring temperatures and increased partitioning of NH₃ into fine particles during this

带格式的: 字体: 倾斜

cooler season. As shown above aerosol-gas partitioning strongly influences NH_3 concentrations; high F_{NH_3} during warm
405 periods, especially summer, favored greater NH_3 gas concentrations due to the thermodynamic tendency for NH_4NO_3 to
dissociate to NH_3 and HNO_3 at high temperature. Although F_{NH_3} was low in winter, indicating NH_4^+ is the dominant NH_x
form in this cold season, winter NH_3 concentrations across all heights still averaged $8.3 \pm 2.6 \mu\text{g m}^{-3}$, with a similar wind
direction distribution as other seasons, except at high altitudes (i.e. 240 m and 320 m, Fig. S6).

5. Conclusions and implications

410 Our study is the first to continually monitor the vertical concentration profile of NH_3 in urban Beijing. Weekly
concentrations were measured for one year at 16 heights on the ~~325-m~~ Beijing 325 m meteorological tower. The NH_3
concentration averaged $13.3 \pm 4.8 \mu\text{g m}^{-3}$. The Highest-highest NH_3 concentrations were always observed at 32-63 m height,
decreasing toward the surface and toward higher altitudes.

NH_3 concentrations at all heights increased during warmer periods, consistent with increased NH_3 emissions under
415 warm conditions and the tendency for semivolatile ammonium nitrate to release NH_3 to the gas phase. Analysis of the
relationship between NH_3 concentrations and local wind direction showed a tendency for higher concentrations during
transport from regions to the south of Beijing, consistent with findings from WPSCF analysis that showed that important
source areas were mainly located to the south of Beijing, consistent with large agricultural regions and high NH_3 emissions
in the North China Plain. Local NH_3 sources, such as urban traffic emissions, may also help account for the elevated NH_3
420 concentrations ($> 5 \mu\text{g m}^{-3}$) observed even in periods when transport came mostly from low NH_3 mountainous regions to
Beijing's north/northwest.

High NH_3 concentrations in urban Beijing, from the surface up to 320 m, the important role that NH_3 plays in $\text{PM}_{2.5}$
and haze formation, and the importance of regional transport of NH_3 emissions from agricultural regions in neighboring
provinces, suggest that future air quality improvement efforts should consider NH_3 emission reductions and that the
425 pollution controls should be jointly practiced at regional scales (e.g. the whole North China Plain) rather than only
controlling local Beijing sources.

Acknowledgements. This work was supported by the State Key Research & Development Programme (2016YFC0207906, 2017YFC0210100, DQGG0208), the National Natural Science Foundation of China (41425007, [91744207](#)), and the National Postdoctoral Program for Innovative Talents (BX201600157).

430 **References**

Ashbaugh, L. L., Malm, W. C., and Sadeh, W. Z.: A residence time probability analysis of sulfur concentrations at Grand Canyon National Park, *Atmos. Environ.* (1967), 19, 1263-1270, [https://doi.org/10.1016/0004-6981\(85\)90256-2](https://doi.org/10.1016/0004-6981(85)90256-2), 1985.

[Baklanov, A. and Kuchin, A.: The mixing height in urban areas: comparative study for Copenhagen, *Atmos. Chem. Phys. Discuss.*, 4, 2839-2866, <https://doi.org/10.5194/acpd-4-2839-2004>, 2004.](#)

435 Bari, A., Ferraro, V., Wilson, L. R., Luttinger, D., and Husain, L.: Measurements of gaseous HONO, HNO₃, SO₂, HCl, NH₃, particulate sulfate and PM_{2.5} in New York, NY, *Atmos. Environ.*, 37, 2825-2835, [https://doi.org/10.1016/S1352-2310\(03\)00199-7](https://doi.org/10.1016/S1352-2310(03)00199-7), 2003.

[Beijing Transport Institute: Annual report of Beijing traffic development in 2017, <http://www.bjtrc.org.cn/JGJS.aspx?id=5.2&Menu=GZCG>, 2017.](#)

440 Chang, Y., Liu, X., Deng, C., Dore, A. J., and Zhuang, G.: Source apportionment of atmospheric ammonia before, during, and after the 2014 APEC summit in Beijing using stable nitrogen isotope signatures, *Atmos. Chem. Phys.*, 16, 11635-11647, <https://doi.org/10.5194/acp-16-11635-2016>, 2016.

Dammers, E., Schaap, M., Haaima, M., Palm, M., Kruit, R. W., Volten, H., Hensen, A., Swart, D., and Erisman, J.: Measuring atmospheric ammonia with remote sensing campaign: Part 1—Characterisation of vertical ammonia concentration profile in the centre of The Netherlands, *Atmos. Environ.*, 169, 97-112, <https://doi.org/10.1016/j.atmosenv.2017.08.067>, 2017.

445 EMEP Webdab emission data hosted by the Centre on Emission Inventories and Projections (CEIP): <http://www.ceip.at>, access: 20 August, 2018⁰⁹.

Erisman, J. W., Vermetten, A. W., Asman, W. A., Waijers-Ijpelaar, A., and Slanina, J.: Vertical distribution of gases and

带格式的: 英语(美国)

- 450 aerosols: the behaviour of ammonia and related components in the lower atmosphere, *Atmos. Environ.* (1967), 22,
1153-1160, [https://doi.org/10.1016/0004-6981\(88\)90345-9](https://doi.org/10.1016/0004-6981(88)90345-9), 1988.
- Erismann, J. W., Sutton, M. A., Galloway, J., Klimont, Z., and Winiwarter, W.: How a century of ammonia synthesis
changed the world, *Nat. Geosci.*, 1, 636-639, <https://doi.org/10.1038/ngeo325>, 2008.
- Fowler, D., Pilegaard, K., Sutton, M., Ambus, P., Raivonen, M., Duyzer, J., Simpson, D., Fagerli, H., Fuzzi, S., and
455 Schjørring, J. K.: Atmospheric composition change: ecosystems-atmosphere interactions, *Atmos. Environ.*, 43,
5193-5267, <https://doi.org/10.1016/j.atmosenv.2009.07.068>, 2009.
- Fu, X., Wang, S., Xing, J., Zhang, X., Wang, T., and Hao, J.: Increasing Ammonia Concentrations Reduce the
Effectiveness of Particle Pollution Control Achieved via SO₂ and NO_x Emissions Reduction in East China, *Environ.*
Sci. Technol. Letters, 4, 221-227, <https://doi.org/10.1021/acs.estlett.7b00143>, 2017.
- 460 Galloway, J. N., Aber, J. D., Erismann, J. W., Seitzinger, S. P., Howarth, R. W., Cowling, E. B., and Cosby, B. J.: The
nitrogen cascade, *AIBS Bulletin*, 53, 341-356, [https://doi.org/10.1641/0006-3568\(2003\)053\[0341:TNC\]2.0.CO;2](https://doi.org/10.1641/0006-3568(2003)053[0341:TNC]2.0.CO;2),
2003.
- Gu, B., Ge, Y., Ren, Y., Xu, B., Luo, W., Jiang, H., Gu, B., and Chang, J.: Atmospheric reactive nitrogen in China:
Sources, recent trends, and damage costs, *Environ. Sci. Technol.*, 46, 9420-9427, <https://doi.org/10.1021/es301446g>,
465 2012.
- Gu, B., Sutton, M. A., Chang, S. X., Ge, Y., and Chang, J.: Agricultural ammonia emissions contribute to China's urban air
pollution, *Front. Ecol. Environ.*, 12, 265-266, <https://doi.org/10.1890/14.WB.007>, 2014.
- Guo, S., Hu, M., Zamora, M. L., Peng, J., Shang, D., Zheng, J., Du, Z., Wu, Z., Shao, M., and Zeng, L.: Elucidating severe
urban haze formation in China, [Proc. Natl. Acad. Sci. USA, Proceedings of the National Academy of Sciences of the
470 United States of America](https://doi.org/10.1073/pnas.1419604111), 111, 17373-17378, <https://doi.org/10.1073/pnas.1419604111>, 2014.
- Huang, R., Zhang, Y., Bozzetti, C., Ho, K., Cao, J., Han, Y., Daellenbach, K. R., Slowik, J. G., Platt, S. M., and Canonaco,
F.: High secondary aerosol contribution to particulate pollution during haze events in China, *Nature*, 514, 218-222,
<https://doi.org/10.1038/nature13774>, 2014.
- Ianniello, A., Spataro, F., Esposito, G., Allegrini, I., Rantica, E., Ancora, M., Hu, M., and Zhu, T.: Occurrence of gas phase

475 ammonia in the area of Beijing (China), *Atmos. Chem. Phys.*, 10, 9487-9503,
<https://doi.org/10.5194/acp-10-9487-2010>, 2010.

Ianniello, A., Spataro, F., Esposito, G., Allegrini, I., Hu, M., and Zhu, T.: Chemical characteristics of inorganic ammonium salts in PM_{2.5} in the atmosphere of Beijing (China), *Atmos. Chem. Phys.*, 11, 10803-10822,
<https://doi.org/10.5194/acp-11-10803-2011>, 2011.

480 Kang, Y., Liu, M., Song, Y., Huang, X., Yao, H., Cai, X., Zhang, H., Kang, L., Liu, X., and Yan, X.: High-resolution ammonia emissions inventories in China from 1980 to 2012, *Atmos. Chem. Phys.*, 16, 2043-2058,
<https://doi.org/10.5194/acp-16-2043-2016>, 2016.

Klimont, Z.: Current and Future Emissions of Ammonia in China, 10th annual emission inventory conference: one atmosphere, One inventory, many challenges, 1-3, May, 2001

485 LeBel, P. J., Hoell, J. M., Levine, J. S., and Vay, S. A.: Aircraft measurements of ammonia and nitric acid in the lower troposphere, *Geophys. Res. Lett.*, 12, 401-404, <https://doi.org/10.1029/GL012i006p00401>, 1985.

Lee, D., Dollard, G., Derwent, R., and Pepler, S.: Observations on gaseous and aerosols components of the atmosphere and their relationships, *Water, Air & Soil Pollut. ion*, 113, 175-202, 1999.

490 Li, P., Yan, R., Yu, S., Wang, S., Liu, W., and Bao, H.: Reinstate regional transport of PM_{2.5} as a major cause of severe haze in Beijing, *Proceedings of the National Academy of Sciences of the United States of America*, 112, E2739-E2740, <https://doi.org/10.1073/pnas.1502596112>, 2015.

Li, Y., Schwandner, F. M., Sewell, H. J., Zivkovich, A., Tigges, M., Raja, S., Holcomb, S., Molenaar, J. V., Sherman, L., and Archuleta, C.: Observations of ammonia, nitric acid, and fine particles in a rural gas production region, *Atmos. Environ.*, 83, 80-89, <https://doi.org/10.1016/j.atmosenv.2013.10.007>, 2014.

495 Li, Y., Thompson, T. M., Damme, M. V., Chen, X., Benedict, K. B., Shao, Y., Day, D., Boris, A., Sullivan, A. P., and Ham, J.: Temporal and spatial variability of ammonia in urban and agricultural regions of northern Colorado, United States, *Atmos. Chem. Phys.*, 17, 6197-6213, <https://doi.org/10.5194/acp-17-6197-2017>, 2017.

Lin, Y., Cheng, M., Ting, W., and Yeh, C.: Characteristics of gaseous HNO₂, HNO₃, NH₃ and particulate ammonium nitrate in an urban city of Central Taiwan, *Atmos. Environ.*, 40, 4725-4733,

500 <https://doi.org/10.1016/j.atmosenv.2006.04.037>, 2006.

[Liu, X., Zhang, Y., Han, W., Tang, A., Shen, J., Cui, Z., Vitousek, P., Erisman, J. W., Goulding K., Christie, P., Fangmeier, A., Zhang, F.: Enhanced nitrogen deposition over China. Nature, 494, 459-462, <https://doi:10.1038/nature11917>, 2013](#)

Meng, Z., Lin, W., Jiang, X., Yan, P., Wang, Y., Zhang, Y., Jia, X., and Yu, X.: Characteristics of atmospheric ammonia over Beijing, China, *Atmos. Chem. Phys.*, 11, 6139-6151, <https://doi.org/10.5194/acp-11-6139-2011>, 2011.

505 Öztürk, F., Bahreini, R., Wagner, N., Dubé, W., Young, C., Brown, S., Brock, C., Ulbrich, I., Jimenez, J., and Cooper, O.: Vertically resolved chemical characteristics and sources of submicron aerosols measured on a Tall Tower in a suburban area near Denver, Colorado in winter, *J. Geophys. Res. [Atmos.]*, 118, 13591-13605, <https://doi.org/10.1002/2013JD019923>, 2013.

510 Pan, Y., Tian, S., Liu, D., Fang, Y., Zhu, X., Gao, M., Gao, J., Michalski, G., and Wang, Y.: Isotopic evidence for enhanced fossil fuel sources of aerosol ammonium in the urban atmosphere, *Environ. Pollut.*, 238, 942-947, <https://doi.org/10.1016/j.envpol.2018.03.038>, 2018a.

Pan, Y., Tian, S., Zhao, Y., Zhang, L., Zhu, X., Gao, J., Huang, W., Zhou, Y., Song, Y., and Zhang, Q.: Identifying ammonia hotspots in China using a national observation network, *Environ. Sci. Technol.*, 52, 3926-3934, <https://doi.org/10.1021/acs.est.7b05235>, 2018b.

515 Plessow, K., Spindler, G., Zimmermann, F., and Matschullat, J.: Seasonal variations and interactions of N-containing gases and particles over a coniferous forest, Saxony, Germany, *Atmos. Environ.*, 39, 6995-7007, <https://doi.org/10.1016/j.atmosenv.2005.07.046>, 2005.

Polissar, A., Hopke, P., Paatero, P., Kaufmann, Y., Hall, D., Bodhaine, B., Dutton, E., and Harris, J.: The aerosol at Barrow, Alaska: long-term trends and source locations, *Atmos. Environ.*, 33, 2441-2458, [https://doi.org/10.1016/S1352-2310\(98\)00423-3](https://doi.org/10.1016/S1352-2310(98)00423-3), 1999.

520 Quan, J., Gao, Y., Zhang, Q., Tie, X., Cao, J., Han, S., Meng, J., Chen, P., and Zhao, D.: Evolution of planetary boundary layer under different weather conditions, and its impact on aerosol concentrations, *Particuology*, 11, 34-40, <https://doi.org/10.1016/j.partic.2012.04.005>, 2013.

带格式的: 字体: 非倾斜, 无下划线

- 525 Reis, S., Pinder, R., Zhang, M., Lijie, G., and Sutton, M.: Reactive nitrogen in atmospheric emission inventories, *Atmos. Chem. Phys.* , 9, 7657-7677, <https://doi.org/10.5194/acp-9-7657-2009>, 2009.
- Riedel, T. P., Wagner, N. L., Dubé, W. P., Middlebrook, A. M., Young, C. J., Öztürk, F., Bahreini, R., VandenBoer, T. C., Wolfe, D. E., and Williams, E. J.: Chlorine activation within urban or power plant plumes: Vertically resolved ClNO₂ and Cl₂ measurements from a tall tower in a polluted continental setting, *J. Geophys. Res. [Atmos.]*, 118, 8702-8715, <https://doi.org/10.1002/jgrd.50637>, 2013.
- 530 Shen, J., Liu, X., Zhang, Y., Fangmeier, A., Goulding, K., and Zhang, F.: Atmospheric ammonia and particulate ammonium from agricultural sources in the North China Plain, *Atmos. Environ.*, 45, 5033-5041, <https://doi.org/10.1016/j.atmosenv.2011.02.031>, 2011.
- Shephard, M., and Cady-Pereira, K.: Cross-track Infrared Sounder (CrIS) satellite observations of tropospheric ammonia, *Atmos. Meas. Tech.*, 8, 1323-1336, <https://doi.org/10.5194/amt-8-1323-2015>, 2015.
- 535 Sun, K., Tao, L., Miller, D. J., Zondlo, M. A., Shonkwiler, K. B., Nash, C., and Ham, J. M.: Open-path eddy covariance measurements of ammonia fluxes from a beef cattle feedlot, *Agric. For. Meteorol.* , 213, 193-202, <https://doi.org/10.1016/j.agrformet.2015.06.007>, 2015.
- Sun, K., Tao, L., Miller, D. J., Pan, D., Golston, L. M., Zondlo, M. A., Griffin, R. J., Wallace, H. W., Leong, Y. J., and Yang, M. M.: Vehicle emissions as an important urban ammonia source in the United States and China, *Environ. Sci. Technol.*, 51, 2472-2481, <https://doi.org/10.1021/acs.est.6b02805>, 2017.
- 540 Sun, Y., Jiang, Q., Wang, Z., Fu, P., Li, J., Yang, T., and Yin, Y.: Investigation of the sources and evolution processes of severe haze pollution in Beijing in January 2013, *J. Geophys. Res. [Atmos.]*, 119, 4380-4398, <https://doi.org/10.1002/2014JD021641>, 2014.
- 545 Sun, Y., Du, W., Fu, P., Wang, Q., Li, J., Ge, X., Zhang, Q., Zhu, C., Ren, L., and Xu, W.: Primary and secondary aerosols in Beijing in winter: sources, variations and processes, *Atmos. Chem. Phys.*, 16, 8309-8329, <https://doi.org/10.5194/acp-16-8309-2016>, 2016.
- Sutton, M. A., Erisman, J. W., Dentener, F., and Möller, D.: Ammonia in the environment: from ancient times to the present, *Environ. Pollut.* , 156, 583-604, <https://doi.org/10.1016/j.envpol.2008.03.013>, 2008.

550 Tang, G., Zhu, X., Hu, B., Xin, J., Wang, L., Münkkel, C., Mao, G., and Wang, Y.: Impact of emission controls on air quality in Beijing during APEC 2014: lidar ceilometer observations, *Atmos. Chem. Phys.*, 15, 12667-12680, <https://doi.org/10.5194/acp-15-12667-2015>, 2015.

[Tang, Y. S., Cape, J. N., and Sutton, M. A.: Development and types of passive samplers for monitoring atmospheric NO₂ and NH₃ concentrations, *Scientific World Journal*, 1, 513-529, <https://doi.org/10.1100/tsw.2001.82>, 2014.](#)

带格式的: 下标

带格式的: 下标

555 Teng, X., Hu, Q., Zhang, L., Qi, J., Shi, J., Xie, H., Gao, H., and Yao, X.: Identification of major sources of atmospheric NH₃ in an urban environment in northern China during wintertime, *Environ. Sci. Technol.*, 51, 6839-6848, <https://doi.org/10.1021/acs.est.7b00328>, 2017.

Tevlin, A., Li, Y., Collett, J., McDuffie, E., Fischer, E., and Murphy, J.: Tall tower vertical profiles and diurnal trends of ammonia in the Colorado Front Range, *J. Geophys. Res. [Atmos.]*, 122, 12468-12487, <https://doi.org/10.1002/2017JD026534>, 2017.

560 [USEPA National Emission Inventory Tier Summaries: <https://www.epa.gov/ttn/chief/eiinformation.html>, access: 14 August 2009](#); [USEPA: Air Pollutant Emissions Trends Data, <https://www.epa.gov/air-emissions-inventories/air-pollutant-emissions-trends-data>, access: 15 October 2018.](#)

Van Damme, M., Clarisse, L., Dammers, E., Liu, X., Nowak, J., Clerbaux, C., Flechard, C., Galy-Lacaux, C., Xu, W., and Neuman, J.: Towards validation of ammonia (NH₃) measurements from the IASI satellite, *Atmos. Meas. Tech.*, 8, 1575-1591, <https://doi.org/10.5194/amt-8-1575-2015>, 2015.

565 VandenBoer, T. C., Brown, S. S., Murphy, J. G., Keene, W. C., Young, C. J., Pszenny, A., Kim, S., Warneke, C., Gouw, J. A., and Maben, J. R.: Understanding the role of the ground surface in HONO vertical structure: High resolution vertical profiles during NACHTT-11, *J. Geophys. Res. [Atmos.]*, 118, 10155-10171, <https://doi.org/10.1002/jgrd.50721>, 2013.

Vogt, E., Held, A., and Klemm, O.: Sources and concentrations of gaseous and particulate reduced nitrogen in the city of Münster (Germany), *Atmos. Environ.*, 39, 7393-7402, <https://doi.org/10.1016/j.atmosenv.2005.09.012>, 2005.

Walker, J., Whittall, D. R., Robarge, W., and Paerl, H. W.: Ambient ammonia and ammonium aerosol across a region of variable ammonia emission density, *Atmos. Environ.*, 38, 1235-1246,

- 575 <https://doi.org/10.1016/j.atmosenv.2003.11.027>, 2004.
- Wang, S., Xing, J., Jang, C., Zhu, Y., Fu, J. S., and Hao, J.: Impact assessment of ammonia emissions on inorganic aerosols in East China using response surface modeling technique, *Environ. Sci. Technol.*, 45, 9293-9300, <https://doi.org/10.1021/es2022347>, 2011.
- Wang, S., Nan, J., Shi, C., Fu, Q., Gao, S., Wang, D., Cui, H., Saiz-Lopez, A., and Zhou, B.: Atmospheric ammonia and its
580 impacts on regional air quality over the megacity of Shanghai, China, *Sci. Rep.*, 5, 15842, <https://doi.org/10.1038/srep15842>, 2015.
- Wang, Y.: MeteInfo: GIS software for meteorological data visualization and analysis, *Meteorological Applications*, 21, 360-368, <https://doi.org/10.1002/met.1345>, 2014.
- Wentworth, G. R., Murphy, J. G., Benedict, K. B., Bangs, E. J., and Collett Jr, J. L.: The role of dew as a night-time
585 reservoir and morning source for atmospheric ammonia, *Atmos. Chem. Phys.*, 16, 7435-7449, <https://doi.org/10.5194/acp-16-7435-2016>, 2016.
- Wiegner, M., Emeis, S., Freudenthaler, V., Heese, B., Junkermann, W., Münkler, C., Schäfer, K., Seefeldner, M., and Vogt, S.: Mixing layer height over Munich, Germany: Variability and comparisons of different methodologies, *J. Geophys. Res. [Atmos.]*, 111, D13201, <https://doi.org/10.1029/2005JD006593>, 2006.
- 590 Wu, Y., Gu, B., Erisman, J. W., Reis, S., Fang, Y., Lu, X., and Zhang, X. PM_{2.5} pollution is substantially affected by ammonia emissions in China, *Environ. Pollut.*, 218, 86-94, <https://doi.org/10.1016/j.envpol.2016.08.027>, 2016
- Wu, Z., Hu, M., Shao, K., and Slanina, J.: Acidic gases, NH₃ and secondary inorganic ions in PM10 during summertime in Beijing, China and their relation to air mass history, *Chemosphere*, 76, 1028-1035, <https://doi.org/10.1016/j.chemosphere.2009.04.066>, 2009.
- 595 Xia, Y., Zhao, Y., and Nielsen, C. P.: Benefits of China's efforts in gaseous pollutant control indicated by the bottom-up emissions and satellite observations 2000–2014, *Atmos. Environ.*, 136, 43-53, <https://doi.org/10.1016/j.atmosenv.2016.04.013>, 2016.
- Xu, W., Luo, X., Pan, Y., Zhang, L., Tang, A., Shen, J., Zhang, Y., Li, K., Wu, Q., Yang, D., Zhang, Y., Xue, J., Li, W., Li, Q., Tang, L., Lu, S., Liang, T., Tong, Y., Liu, P., Zhang, Q., Xiong, Z., Shi, X., Wu, L., Shi, W., Tian, K., Zhong,

- 600 X., Shi, K., Tang, Q., Zhang, L., Huang, J., He, C., Kuang, F., Zhu, B., Liu, H., Jin, X., Xin, Y., Shi, X., Du, E., Dore,
A. J., Tang, S., Collett Jr., J. L., Goulding, K., Sun, Y., Ren, J., Zhang, F., and Liu, X.: Quantifying atmospheric
nitrogen deposition through a nationwide monitoring network across China, *Atmos. Chem. Phys.*, 15, 12345-12360,
<https://doi.org/10.5194/acp-15-12345-2015>, 2015.
- Xu, W., Song, W., Zhang, Y., Liu, X., Zhang, L., Zhao, Y., Liu, D., Tang, A., Yang, D., Wang, D., Wen, Z., Pan, Y.,
605 Fowler, D., Collett Jr., J. L., Erisman, J. W., Goulding, K., Li, Y., and Zhang, F.: Air quality improvement in a
megacity: implications from 2015 Beijing Parade Blue pollution control actions, *Atmos. Chem. Phys.*, 17, 31-46,
<https://doi.org/10.5194/acp-17-31-2017>, 2017.
- Yamamoto, N., Kabeya, N., Onodera, M., Takahahi, S., Komori, Y., Nakazuka, E., and Shirai, T.: Seasonal variation of
atmospheric ammonia and particulate ammonium concentrations in the urban atmosphere of Yokohama over a 5-year
610 period, *Atmos. Environ.* (1967), 22, 2621-2623, [https://doi.org/10.1016/0004-6981\(88\)90498-2](https://doi.org/10.1016/0004-6981(88)90498-2), 1988.
- Yamamoto, N., Nishiura, H., Honjo, T., Ishikawa, Y., and Suzuki, K.: A long-term study of atmospheric ammonia and
particulate ammonium concentrations in Yokohama, Japan, *Atmos. Environ.*, 29, 97-103,
[https://doi.org/10.1016/1352-2310\(94\)00226-B](https://doi.org/10.1016/1352-2310(94)00226-B), 1995.
- Yang, F., Tan, J., Zhao, Q., Du, Z., He, K., Ma, Y., Duan, F., Chen, G., and Zhao, Q.: Characteristics of PM_{2.5} speciation
615 in representative megacities and across China, *Atmos. Chem. Phys.*, 11, 5207-5219,
<https://doi.org/10.5194/acp-11-5207-2011>, 2011.
- Ye, X., Ma, Z., Zhang, J., Du, H., Chen, J., Chen, H., Yang, X., Gao, W., and Geng, F.: Important role of ammonia on
haze formation in Shanghai, *Environ. Res. Lett.*, 6, 024019, <https://doi.org/10.1088/1748-9326/6/2/024019>, 2011.
- Zbieranowski, A. L., and Aherne, J.: Spatial and temporal concentration of ambient atmospheric ammonia in southern
620 Ontario, Canada, *Atmos. Environ.*, 62, 441-450, <https://doi.org/10.1016/j.atmosenv.2012.08.041>, 2012.
- Zhang, L., Wright, L., and Asman, W.: Bi-directional air-surface exchange of atmospheric ammonia: A review of
measurements and a development of a big-leaf model for applications in regional-scale air-quality models, *J. Geophys.
Res. [Atmos.]*, 115, D20310, <https://doi.org/10.1029/2009JD013589>, 2010.
- Zhang, L., Chen, Y., Zhao, Y., Henze, D. K., Zhu, L., Song, Y., Paulot, F., Liu, X., Pan, Y., and Lin, Y.: Agricultural

- 625 ammonia emissions in China: reconciling bottom-up and top-down estimates, *Atmos. Chem. Phys.*, 18, 339-355,
<https://doi.org/10.5194/acp-18-339-2018>, 2018.
- Zhang, Q., Streets, D. G., Carmichael, G. R., He, K., Huo, H., Kannari, A., Klimont, Z., Park, I. S., Reddy, S., Fu, J., Chen,
D., Duan, L., Lei, Y., Wang, L., and Yao, Z.: Asian emissions in 2006 for the NASA INTEX-B mission, *Atmos.*
Chem. Phys., 9, 5131-5153, <https://doi.org/10.5194/acp-9-5131-2009>, 2009.
- 630 Zhang, X., Wu, Y., Liu, X., Reis, S., Jin, J., Dragosits, U., Damme, M. V., Clarisse, L., Whitburn, S., Coheur, P. F., and
Gu, B.: Ammonia emissions may be substantially underestimated in China, *Environ. Sci. Technol.*, 51, 12089-12096,
<https://doi.org/10.1021/acs.est.7b02171>, 2017.
- Zhang, Y., Dore, A. J., Ma, L., Liu, X., Ma, W., Cape, J.N., and Zhang, F.: Agricultural ammonia emissions inventory and
spatial distribution in the North China Plain. *Environ. Pollut.*, 158, 490-501,
635 <https://doi.org/10.1016/j.envpol.2009.08.033>, 2010.
- Zhao, D., and Wang, A.: Estimation of anthropogenic ammonia emissions in Asia, *Atmos. Environ.*, 28, 689-694,
[https://doi.org/10.1016/1352-2310\(94\)90045-0](https://doi.org/10.1016/1352-2310(94)90045-0), 1994.
- Zhao, X., Zhang, X., Xu, X., Xu, J., Meng, W., and Pu, W.: Seasonal and diurnal variations of ambient PM_{2.5}
concentration in urban and rural environments in Beijing, *Atmos. Environ.*, 43, 2893-2900,
640 <https://doi.org/10.1016/j.atmosenv.2009.03.009>, 2009.
- Zheng, G., Duan, F., Su, H., Ma, Y., Cheng, Y., Zheng, B., Zhang, Q., Huang, T., Kimoto, T., Chang, D., Pöschl, U.,
Cheng, Y., and He, K.: Exploring the severe winter haze in Beijing: the impact of synoptic weather, regional transport
and heterogeneous reactions, *Atmos. Chem. Phys.*, 15, 2969-2983, <https://doi.org/10.5194/acp-15-2969-2015>, 2015.
- Zhou, Y., Zhu, X., Pan, Y., Tian, S., Liu, Q., Sun, Y., An, J., and Wang, Y.: Vertical distribution of gaseous pollutants in
645 the lower atmospheric boundary layer in urban Beijing, *Environmental Chemistry (in Chinese)*, 36, 1752-1759, 2017.

Table 1 Overview of measured vertical NH₃ concentration (μg m⁻³) in previous studies and this study.

Heights (m) / NH ₃ (μg m ⁻³)	Netherlands		US BAO tower	Beijing IAS tower	
	Rural area	Meteorological tower			
0~5	6.8 (1_m)	8.3	4.7	=	12.5
	6.5 (4_m)				
5~10	-	-	5.0	<u>7.9</u>	13.4
10~20	9.6	-	-	<u>15.8</u>	13.8
20~40	-	6.2	4.61	=	14.2
40~60	-	-	4.19	<u>12.8</u>	14.1
60~80	-	-	-	<u>12.5 (80 m)</u>	<u>14.3 (63 m)</u>
					<u>14.2 (80 m)</u>
80~100	-	3.6	3.6	=	13.9
100~150	-	-	3.09	<u>12.4 (120 m)</u>	14.0 (120_m)
					13.8 (140_m)
					13.5 (160_m)
150~200	4.5	2.1	2.72	<u>14.0 (160 m)</u>	13.3 (180_m)
				<u>6.7 (200 m)</u>	12.7 (200_m)
200~250	-	-	2.39	<u>9.1</u>	12.1
250~300	-	-	2.25	<u>7.3</u>	11.8
300~350	-	-	-	<u>7.6</u>	11.3
Period	2014		12/13/2011–1/9/2013	<u>2/10/2009-2/25/2009</u>	3/16/2016–3/16/2017
References	Dammers et al. (2017)	Erisman et al. (1988)	Li et al. (2017)	<u>Zhou et al. (2017)</u>	This study

带格式表格

带格式表格

带格式表格

带格式的：字体颜色：自动设置

带格式的：字体颜色：自动设置

带格式的：字体颜色：自动设置

带格式表格

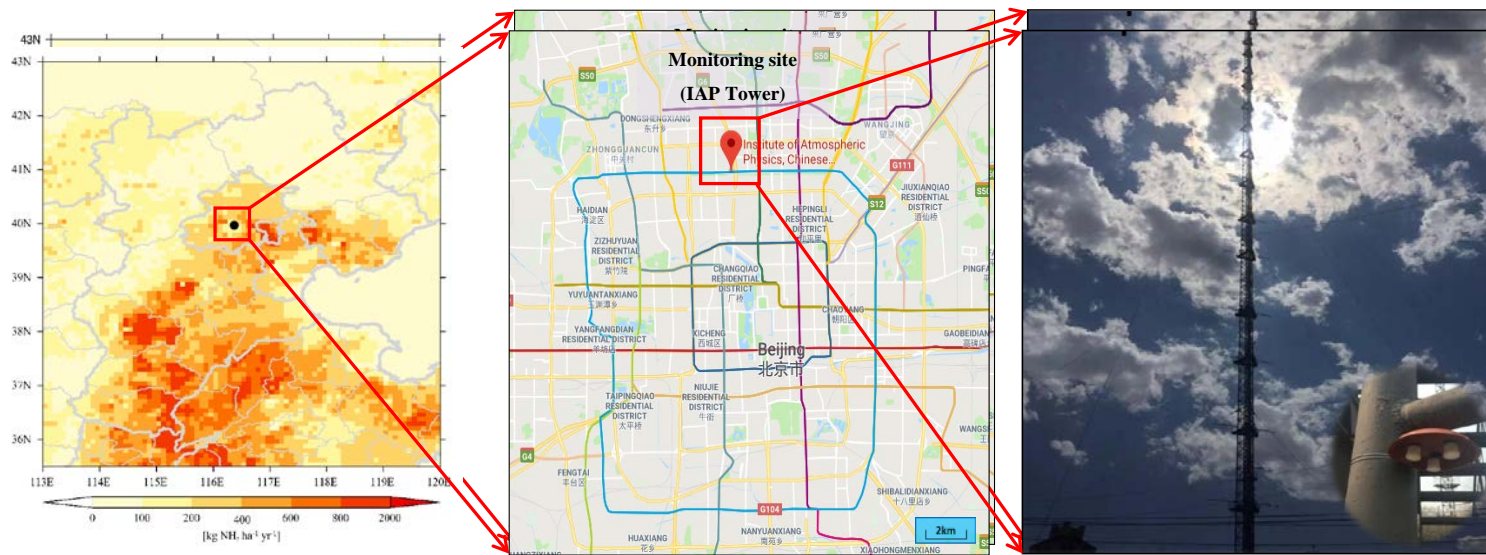


Fig. 1 Left: Modeled NH₃ emissions distribution (0.1°, ~10 km) over North China Plain in 2015 with the location of the monitoring site shown as a black dot. NH₃ emission estimates are from the inventory of Zhang et al. (2018) at 0.1° horizontal resolution. Right: Map of Beijing showing the location of the monitoring tower.

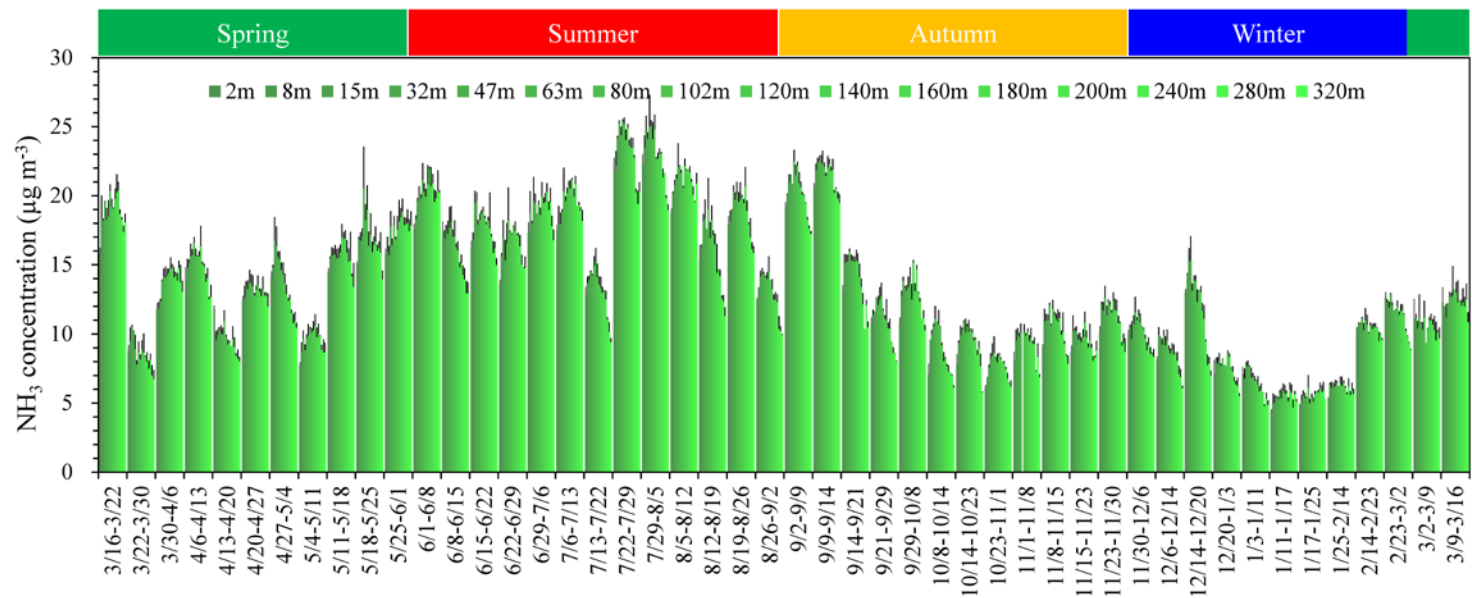
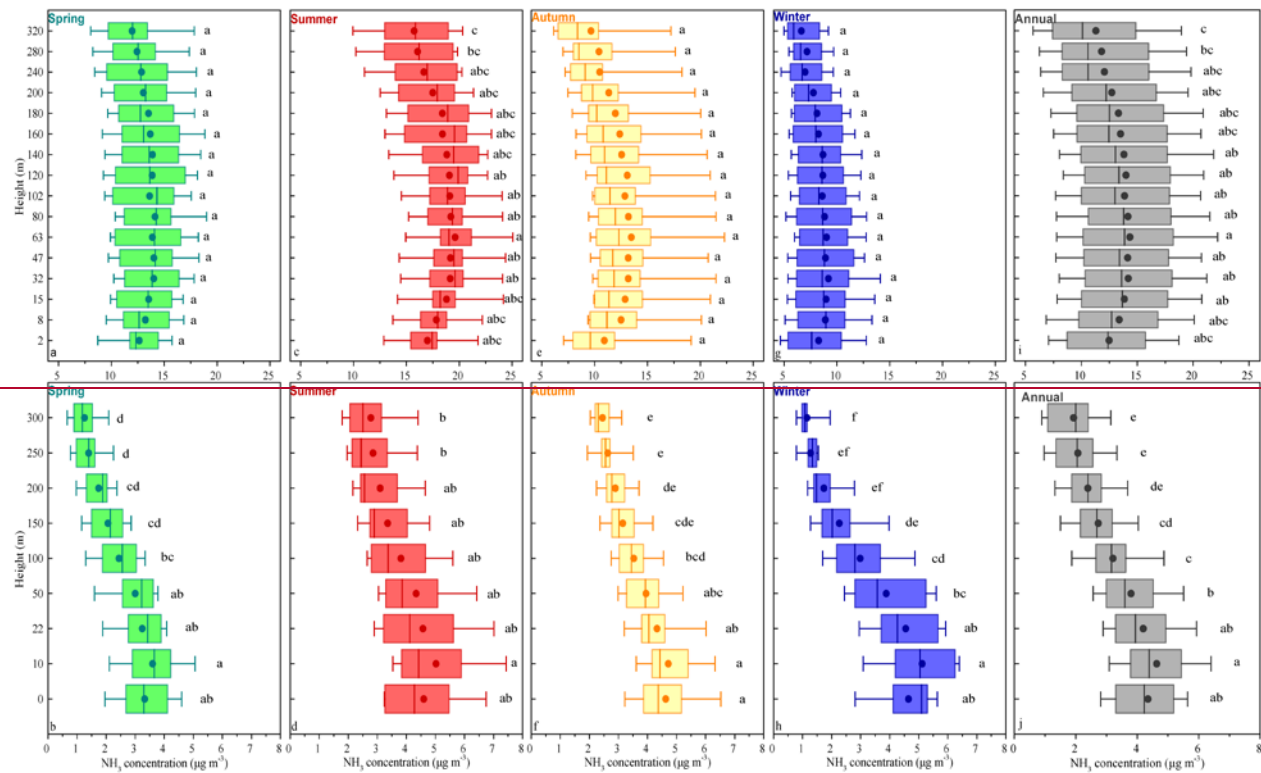


Fig. 2 Time series of vertical distribution of weekly atmospheric NH₃ concentrations ($\pm\sigma$) in Beijing urban (03/16/2016 - 03/16/2017)



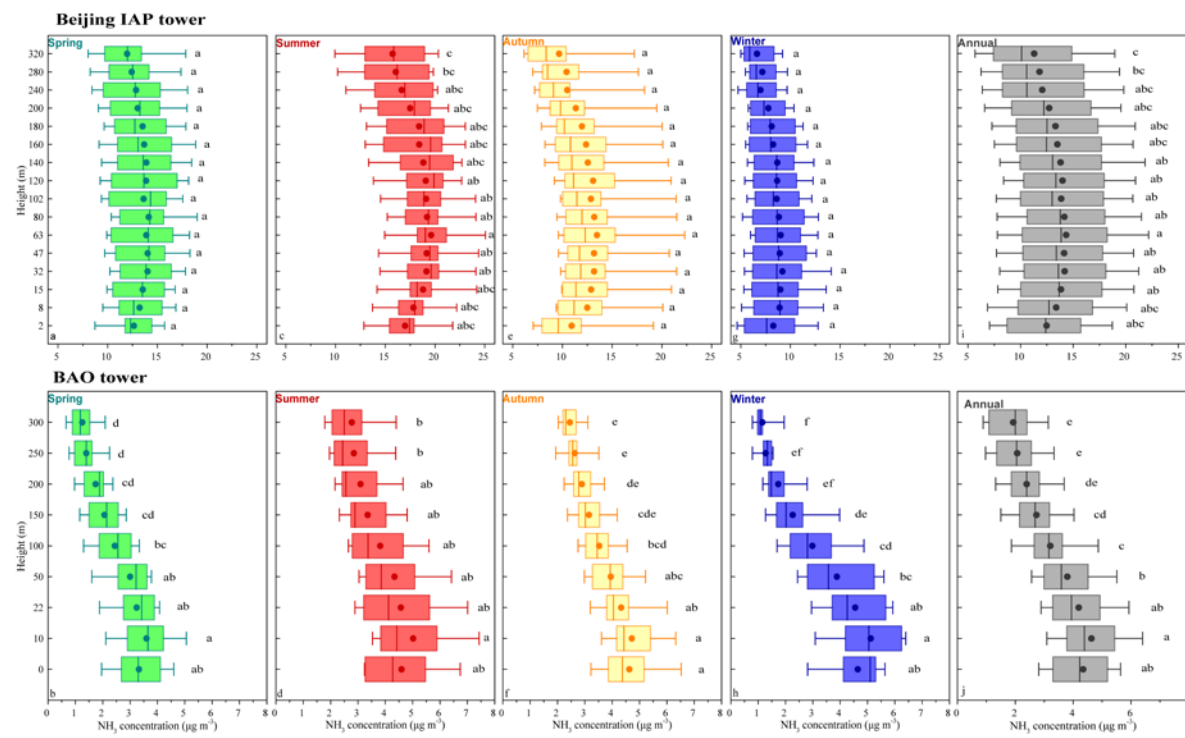


Fig. 3 Comparison of seasonal vertical NH₃ concentrations with the mean (dots), median, 10th, 25th, 75th and 90th percentiles of the NH₃ concentrations of each height for IAP tower (Beijing, this study) (fig. a, c, e, g, i) and BAO tower (USA, Li et al., 2017) (fig. b, d, f, h, j).

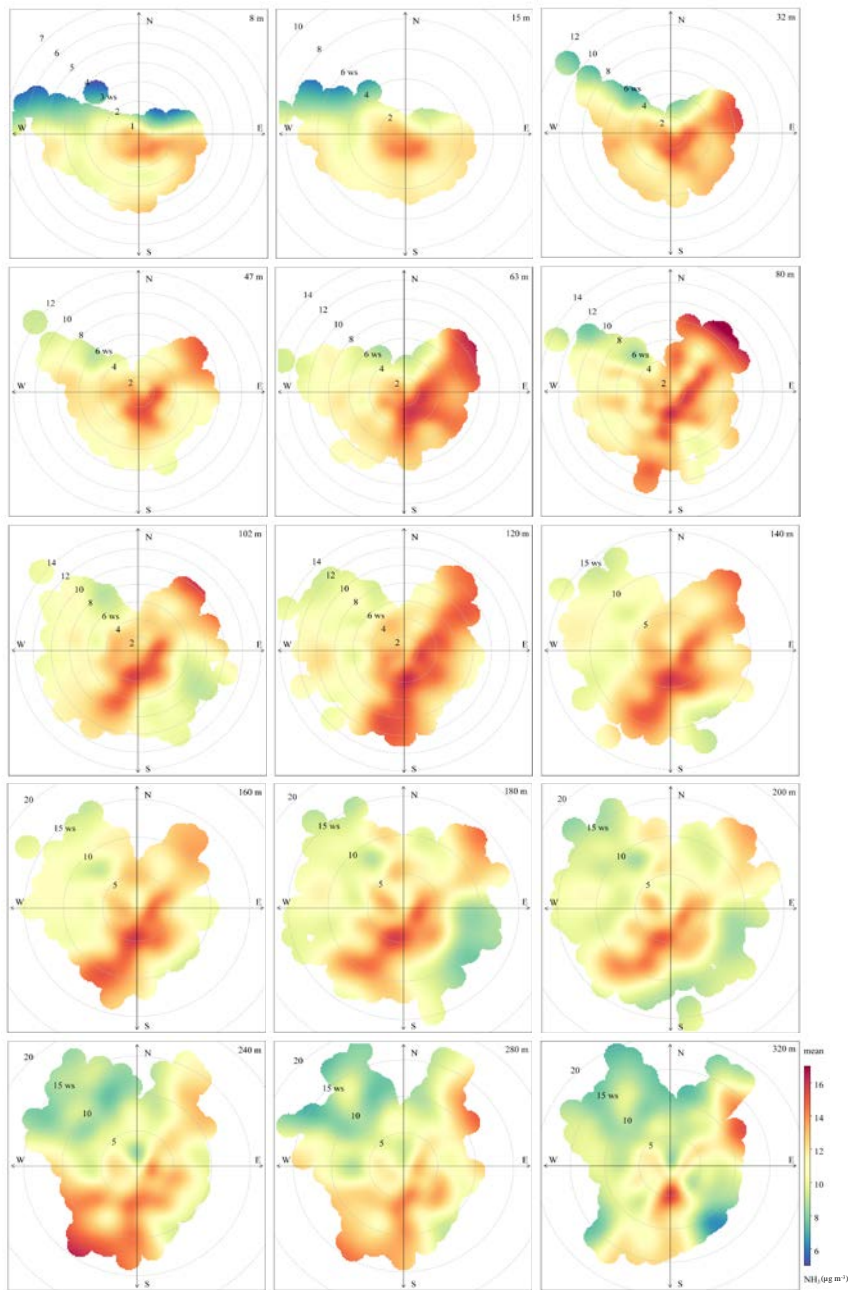


Fig. 4 The frequency distributions of wind directions and NH_3 concentration (color demarcation) for all height during the observation period. Radial data are WS (m s^{-1}) as a function of WD ($^\circ$), The colors denote the NH_3 concentrations ($\mu\text{g m}^{-3}$).

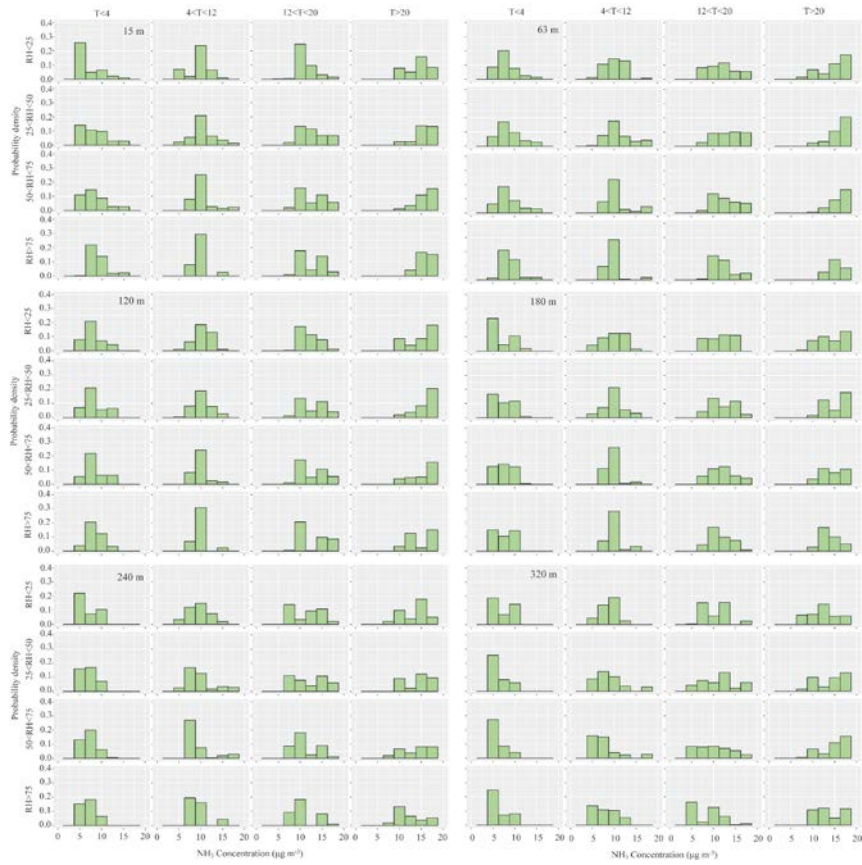


Fig. 5 Probability density of NH₃ concentration ($\mu\text{g m}^{-3}$) at different ranges of temperature* ($^{\circ}\text{C}$) and relative humidity* (%) for 14 heights.

* Temperature includes four subsets: <4 $^{\circ}\text{C}$, 4-12 $^{\circ}\text{C}$, 12-20 $^{\circ}\text{C}$ and >20 $^{\circ}\text{C}$;

* Relative humidity includes four subsets: <25%, 25-50%, 50-75% and >75%.

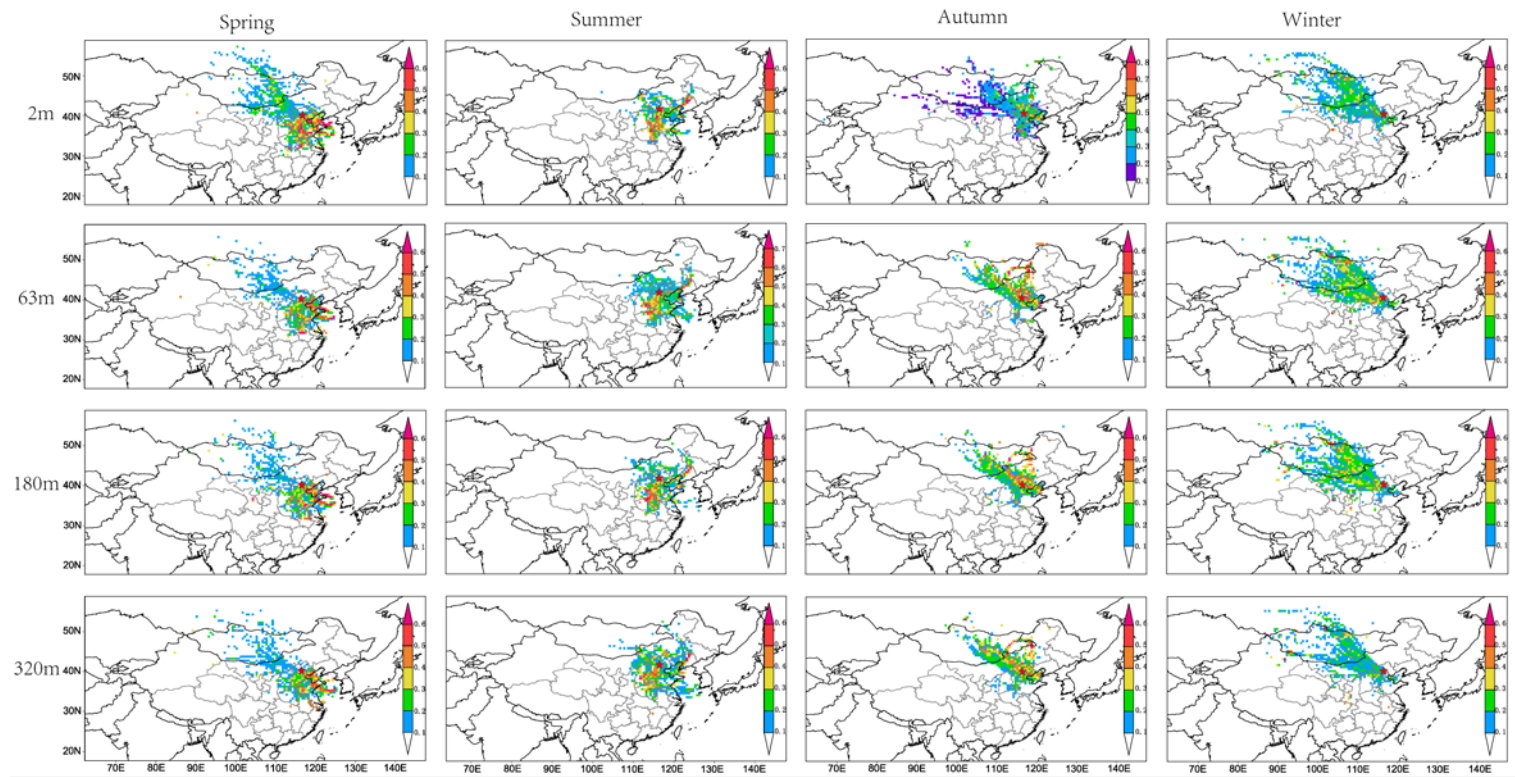


Fig. 6 Weighted potential source contribution analysis (WPSCF) of atmospheric NH₃ in Beijing during 03/16/2016 – 03/16/2017.